Fusion Based Gaussian noise Removal in the Images Using Curvelets and Wavelets With Gaussian Filter

NAGA SRAVANTHI KOTA *nagasravanthi.kota@gmail.com*
Department of Electronics and Communication Engineering
Sri Venkateswara University
Tirupati - 517 502, India.

G. UMAMAHESWARA REDDY *umaskit@gmail.com*
Department of Electronics and Communication Engineering
Sri Venkateswara University
Tirupati - 517 502, India

Abstract

Denoising images using Curvelet transform approach has been widely used in many fields for its ability to obtain high quality images. Curvelet transform is superior to wavelet in the expression of image edge, such as geometry characteristic of curve, which has been already obtained good results in image denoising. However artifacts those appear in the result images of Curvelets approach prevent its application in some fields such as medical image. This paper puts forward a fusion based method using both Wavelets and Curvelet transforms because certain regions of the image have the ringing and radial stripe after Curvelets transform. The experimental results indicate that fusion method has an abroad future for eliminating the noise of images. The results of the algorithm applied to ultrasonic medical images indicate that the algorithm can be used efficiently in medical image fields also.

Keywords: Gaussian Filtering, Wavelet Transform, Curvelets Transform, Image Fusion, Denoising.

1. INTRODUCTION

Sparse representation of image data, where most of the information is packed into small number of data, is very important in many image processing applications. Image denoising using wavelets has been widely used in recent years and provides better accuracy in denoising different types of images. Wavelets are suitable for dealing with objects with point singularities. Wavelets can only capture limited directional information due to its poor orientation selectivity. By decomposing the image into a series of high-pass and low-pass filter bands, the wavelet transform extracts directional details that capture horizontal, vertical, and diagonal activity. However, these three linear directions are limiting and might not capture enough directional information in noisy images, such as medical Magnetic Resonance Images, which do not have strong horizontal, vertical, or diagonal directional elements. Wavelets provide a very sparse and efficient representation for piecewise smooth signals, but it cannot efficiently represent discontinuities along edges or curves in images or objects.

Ridgelet improves denoising; however, they capture structural information of an image based on multiple radial directions in the frequency domain. Line singularities in ridgelet transform provides better edge detection than its wavelet counterpart. One limitation to use ridgelet in image denoising is that ridgelet is most effective in detecting linear radial structures, which are not dominant in medical images. Due to the above-mentioned shortcoming of wavelet transform, Donoho and others proposed Curvelet transform theory and their anisotropy character is very useful for the efficient expression of image edges and gets good results in image denoising. The curvelet transform is a recent extension of ridgelet transform that overcome ridgelet weaknesses in medical image denoising. Curvelet is proven to be particularly effective at detecting image activity along curves instead of radial directions which are the most comprising objects of medical images. However, Curvelet transform for denoising has also brought some negative impacts shows that it appears slightly “scratches” and “ringing” phenomenon in the reconstructed image, due to this situation, we have proposed fusion based method using images reconstructed from wavelet transform, curvelets transform and Gaussian filter for image denoising.

2. DENOISING METHODS

2.1 Gaussian Filtering

2D Gaussian filters are useful to provide image smoothing with minimal computations. Smoothing can reduce high frequency noise in an image while creating an image where a pixel and its neighbors are correlated with each other. Gaussian filters are able to smooth images with minimal computations because they are separable. This means that instead of using a 2D filter you can for example apply a 1D filter along the x-axis of the image and another 1D filter along the image's y-axis.

From a linear algebra perspective separable filters exploit the fact that the 2D Gaussian filter is really a rank one outer product of the two 1D filters. A 2D filter is only separable if it is aligned with the image axis and centered at the origin. In two-dimensions, one can vary a Gaussian in more parameters: not only may one vary a single width, but one may vary two separate widths, and rotate: one thus obtains both circular Gaussians and elliptical Gaussians, accordingly as the level sets are circles or ellipses. A particular example of Gaussian function is

$$f(x, y) = A e^{\left(\frac{(x-x_0)^2}{2\sigma_x^2} + \frac{(y-y_0)^2}{2\sigma_y^2} \right)} \quad (1)$$

Here the coefficient *A* is the amplitude, x_o, y_o is the center and σ_x, σ_y are the *x* and *y* spreads of the blob.

2.2 Wavelet Thresholding Using Bayesshrink

Chang et al. proposed the BayesShrink scheme. In BayesShrink we determine the threshold for each Subband assuming a **Generalized Gaussian distribution (GGD**) [1] .The GGD is given by

$$GG_{\sigma_X,\beta}(x) = C(\sigma_X, \beta)\exp-[\alpha(\sigma_X, \beta)|x|]^{\beta} \quad (2)$$

$-\infty < x < \infty, \sigma_X > 0, \beta > 0$ Where

$$\alpha(\sigma_X, \beta) = \sigma_X^{-1}\left[\frac{\Gamma(3/\beta)}{\Gamma(1/\beta)}\right]^{1/2} \quad (3)$$

$$C(\sigma_X, \beta) = \frac{\beta.\alpha(\sigma_X, \beta)}{2\Gamma(1/\beta)}$$ and

$$\Gamma(t) = \int_0^{\infty} e^{-u}u^{t-1}du$$

The parameter σ_X is the standard deviation and β is the shape parameter. β ranges from 0.5 to 1. Assuming such a distribution for the wavelet coefficients, we empirically estimate β and σ_X for each subband and try to find the threshold *T* which minimizes the Bayesian Risk, i.e. the expected value of the mean square error.

$$\tau(T) = \mathrm{E}(\hat{X} - X)^2 = \mathrm{E}_X \mathrm{E}_{Y/X} (\hat{X} - X)^2 \qquad (4)$$

Where $\hat{X} = \eta_T(Y), Y/X \sim N(x, \sigma^2)$ and $X \sim GG_{\sigma_X, \beta}$ the optimal threshold T^* is then given by

$$T^*(\sigma_X, \beta) = \arg\min_T \tau(T) \qquad (5)$$

This is a function of the parameters σ_X and β. since there is no closed form solution for T^*,numerical calculation is used to find its value. It is observed that the threshold value set by

$$T_B(\sigma_X) = \frac{\sigma^2}{\sigma_X} \qquad (6)$$

is very close to T^*

The estimated threshold $T_B = \sigma^2 / \sigma_X$ is not only nearly optimal but also has an intuitive appeal. When $\sigma / \sigma_X << 1$, the signal is much stronger than the noise, T_B / σ is chosen to be small in order to preserve most of the signal and remove some of the noise, when $\sigma / \sigma_X >> 1$, the noise dominates and the normalized threshold is chosen to be large to remove the noise which has overwhelmed the signal. Thus, this threshold choice adapts to both the signal and the noise characteristics as reflected in the parameters σ and σ_X

Parameter Estimation to determine the threshold: The GGD parameters, σ_X and β need to be estimated to compute $T_B(\sigma_X)$.The noise variance σ^2 is estimated from the subband HH_1 by the robust median estimator.

$$\hat{\sigma} = \frac{Median\left(\left|Y_{ij}\right|\right)}{0.6745}, Y_{ij} \in \text{subband HH1.}$$

The observation model is *Y = X + V,* with *X* and *V* independent of each other, hence

$$\sigma_Y{}^2 = \sigma_X{}^2 + \sigma^2 \qquad (7)$$

With $\sigma_Y{}^2$ is the variance of *Y.* since *Y* is modeled as zero-mean, $\sigma_Y{}^2$ can be found empirically by

$$\hat{\sigma}_Y{}^2 = \frac{1}{n^2} \sum_{i,j=1}^{n} Y_{ij}{}^2 \qquad (8)$$

Where (n x n) is the size of the subband under consideration. Thus

$$\hat{T}_B(\hat{\sigma}_X) = \frac{\hat{\sigma}^2}{\hat{\sigma}_X} \qquad (9)$$

Where

$$\hat{\sigma}_X = \sqrt{\max\left(\hat{\sigma}_Y{}^2 - \hat{\sigma}^2, 0\right)} \qquad (10)$$

In the case that $\hat{\sigma}^2 \geq \hat{\sigma}_Y{}^2$, $\hat{\sigma}_X$ is taken to be zero i.e. $\hat{T}_B(\hat{\sigma}_X)$ is ∞ or in practice, $\hat{T}_B(\hat{\sigma}_X) = \max\left(\left|Y_{ij}\right|\right)$ and all coefficients are set to zero.

2.3 Curvelet Transform

Curvelet transform is proposed by Candes and Donoho in 1999, its essence is derived from the ridge-wave theory [2]. In the foundation of single ridge-wave or local ridge-wave transform, we can construct Curvelet to express the objects which have curved singular boundary, Curvelet combines the advantages of ridge-wave which is suitable for expressing the lines' character and wavelet which is suitable for expressing the points' character and take full advantage of multi-scale analysis, it is suitable for a large class of image processing problems and has got quite good results in practical application [3]. Curvelet transform develops from 1999 until now, has transformed from the first generation (J.L.Starck, 2002) to the second generation theory (E.J.Candes, 2005) [4]. Based on this, research scholars realize the conversion process more simply and quickly, they develop another new algorithm. The first method is based on unequally-spaced fast Fourier transforms (USFFT) and the second is based on the wrapping of specially selected Fourier samples. The two implementations essentially differ by the choice of spatial grid used to translate Curvelets at each scale and angle. The 'wrapping' approach used in this paper assumes the same digital coronization as digital curvelet transform theory, but makes a different, somewhat simpler choice of spatial grid to translate Curvelets at each scale and angle[6]. Instead of a tilted grid, we assume a regular rectangular grid and define 'Cartesian' Curvelets in essentially the same way as before,

$$c(j,l,k) = \int \hat{f}(\omega)\tilde{U}_j(S_{\theta_1}^{-1}\omega)e^{i\langle b,\omega\rangle}d\omega \tag{11}$$

Discrete curvelet transform formula

$$c(j,l,k) = \int \hat{f}(\omega)\tilde{U}_j(S_{\theta_1}^{-1}\omega)e^{i\langle S_{\theta_1}^{-T}b,\omega\rangle}d\omega \tag{12}$$

Notice that $S_{\theta_1}^{-T}b$ has been replaced by $b \simeq (k_1 2^{-j}, k_2 2^{-\frac{j}{2}})$ taking on values on a rectangular grid. As before, this formula for b is understood When $\theta \in \left(\frac{-\pi}{4}, \frac{\pi}{4}\right)$ or $\theta \in \left(\frac{3\pi}{4}, \frac{5\pi}{4}\right)$.

Wrapping round origin point is the core of Wrapping based curvelet. It realizes one to one through the periodization technology in the affine region. As shown in figure 1, Curvelet's essence is multi-scale localized ridge-wave, Curvelet transform is localized multi- scale ridge-wave transform, in fact. Curvelet's decomposition includes the following steps:

1) Sub-band decomposition: use wavelet transforms to the image and decomposes it to multiple sub-band components;
2) Smooth segmentation:" smooth segment" every subband to some sub-blocks, the size of the sub-blocks after each scale's division can be determined according to specific needs and can be different each other.
3) Ridge-wave analysis: make localized ridge-wave transform to each sub-blocks after segmentation.

Practice has proved that traditional Curvelet transform method has the phenomenon that it would appear slightly "scratches" and "ringing" in the image which is dialed with by denoising and reconstruction.

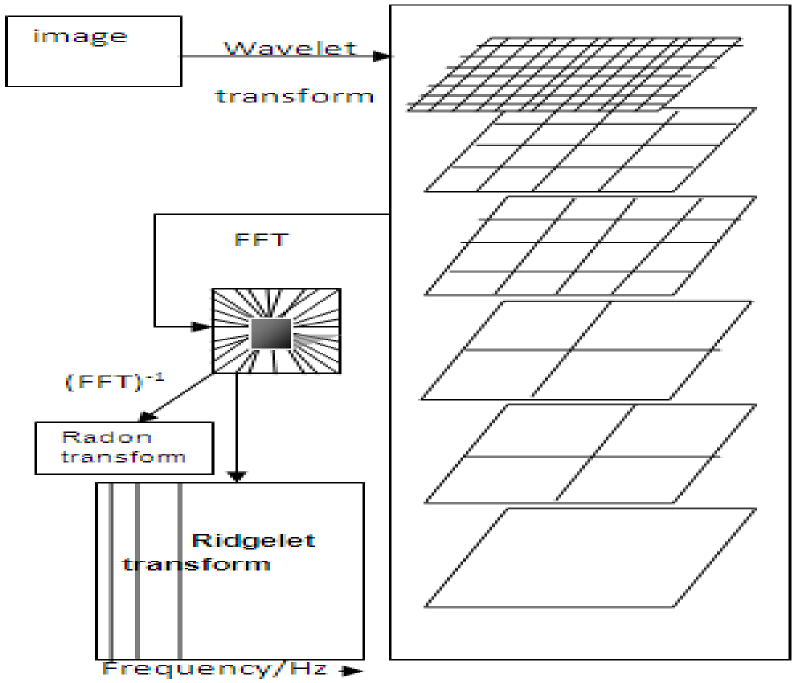

FIGURE1 . Curvelet transform

2.4 Proposed Method

The image contains a variety of areas, such as texture region, smooth region and so on; these different areas have different tolerances to the noise. If we use the same processing method with no difference, the consequences are filtering too much detailed information and damaging the detailed information of the edge or the edges are protected but to retain too much noise or it may cause a variety of distortions. The traditional Curvelet transform has the problem, has the phenomenon that it would appear slightly “scratches” and “ringing” in the image which is dialed with by denoising and reconstruction. To solve this problem, we can make the improvement, the steps are as follows:

1) Use Gaussian filtering on the noisy image and obtain the reconstructed image.
2) Use two-dimensional wavelet to denoise the original image which concludes noise.
3) Use Curvelet transform to denoise the original image which concludes noise.
4) Fusion the images which are processed by step (1),step(2) and step(3) , we can obtain better denoised image.

3. RESULTS AND DISCUSSIONS

This Denoising is carried out for the three standard gray scale images like Lena, house and boat of size 512x512, peppers colour image and also one MRI image of size 512x512 taken from the Visible Human Male data set of visible human project, released in November 1994.Then denoising is performed on these images corrupted with white Gaussian noise. To evaluate our method, we use the Peak Signal to Noise Ratio *(PSNR)*, which is defined as:

$$PSNR = 10\log_{10}\left(\frac{255^2}{MSE}\right) \tag{13}$$

Where *MSE* is the Mean Square Error:

$$MSE = \frac{1}{MN}\sum_{m=0}^{M-1}\sum_{n=0}^{N-1}\left|x(m,n) - \hat{x}(m,n)\right|^2 \tag{14}$$

Where M and N are the number of lines and columns of the image, $x(m,n)$ and $\hat{x}(m,n)$ are the pixels of the original and the processed image. However, the PSNR do not correlate well with subjective quality evaluation. In fact, the HVS is sensitive to the noise on the uniform zones. Its perception on the textured zones is more difficult. To take in account this characteristic of the HVS, we use the weighted PSNR *(WPSNR)* that use the local variance of the image to ponder the error:

$$WPSNR = 10\log_{10}\left(\frac{255^2}{wMSE}\right) \tag{15}$$

Where

$$WMSE = \frac{1}{MN}\sum_{m=0}^{M-1}\sum_{n=0}^{N-1}\left|\frac{x(m,n) - \hat{x}(m,n)}{I + \mathrm{var}(m,n)}\right|^2 \tag{16}$$

image	sigma(dB)	Gaussian filtering	Wavelet Transform denoising	Curvelet Transform denoising	fusion based denoising
MRI	30	34.2372	34.6475	34.7834	35.2639
"	50	30.0025	30.7335	30.7855	31.1393
LENA	30	36.0373	36.8384	37.5526	38.093
"	50	32.0341	33.5867	34.0649	34.6634
BOAT	30	35.488	35.8198	35.8387	36.6309
"	50	31.7195	32.4621	32.414	33.2787
HOUSE	30	36.3317	37.7527	38.6751	39.1076
"	50	32.2772	34.9115	35.4168	35.8162

TABLE 1: List of WPSNR values for images denoised from four denoising methods for four standard images corrupted by Gaussian noise of standard deviations σ =30 and σ =50

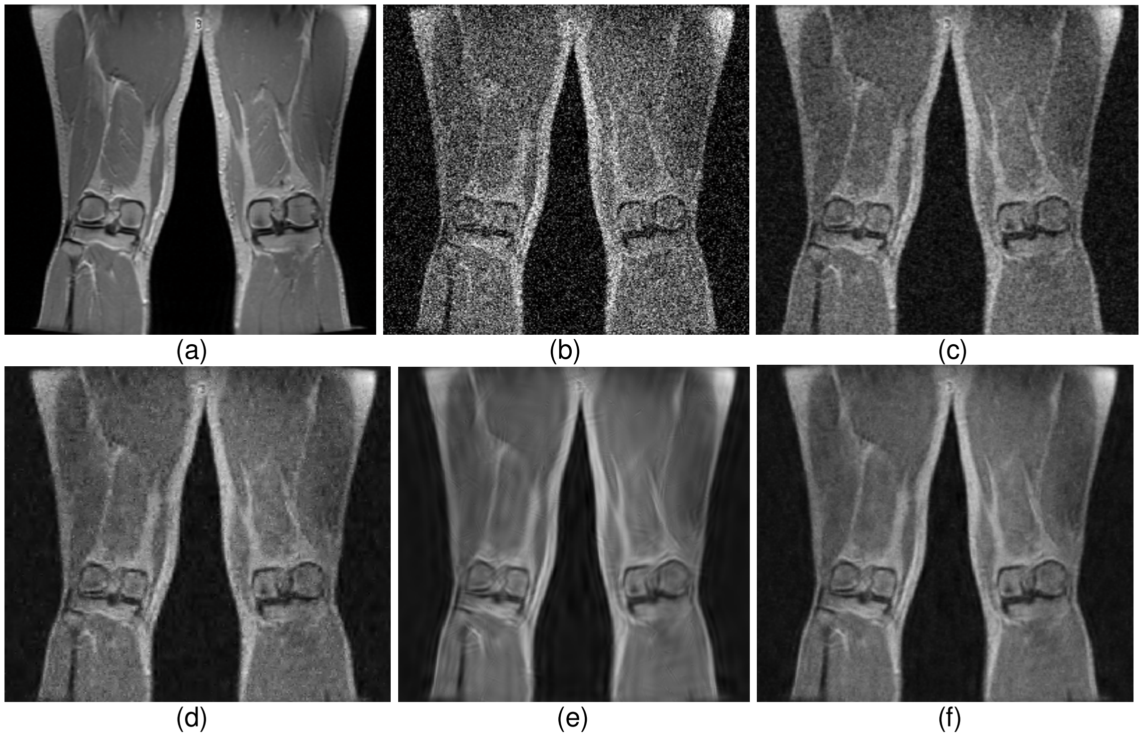

FIGURE 2: MRI test image: (a) Original image, (b) Noisy image with σ = 50 dB, (c) Image after denoising with Gaussian filter , (d) Denoised image from BayesShrink Wavelet Thresholding, (e)Denoised image from Curvelet transform, (f)Denoised image from Proposed method.

FIGURE 3: GIRL test image: (a) Original image, (b) Noisy image with σ = 50 dB, (c) Image after denoising with Gaussian filter , (d) Denoised image from BayesShrink Wavelet Thresholding, (e)Denoised image from Curvelet transform, (f)Denoised image from Proposed method.

FIGURE 4: Lena colour test image: (a) Original image, (b) Noisy image with σ = 50 dB, (c) Image after denoising with Gaussian filter , (d) Denoised image from BayesShrink Wavelet Thresholding, (e)Denoised image from Curvelet transform, (f)Denoised image from Proposed method.

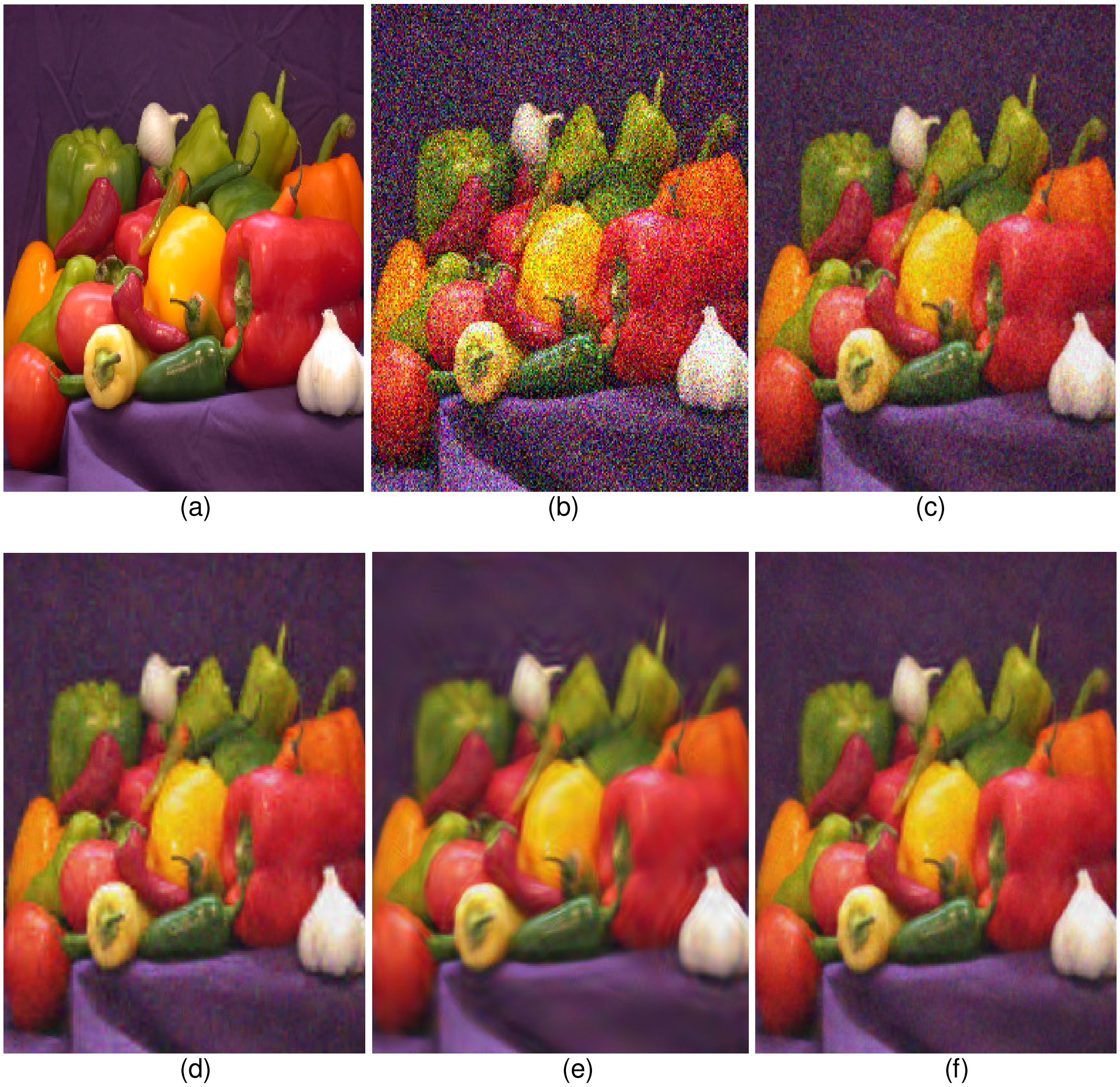

FIGURE 5: Peppers colour test image: (a) Original image, (b) Noisy image with σ = 50 dB, (c) Image after denoising with Gaussian filter , (d) Denoised image from BayesShrink Wavelet Thresholding, (e)Denoised image from Curvelet transform, (f)Denoised image from Proposed method.

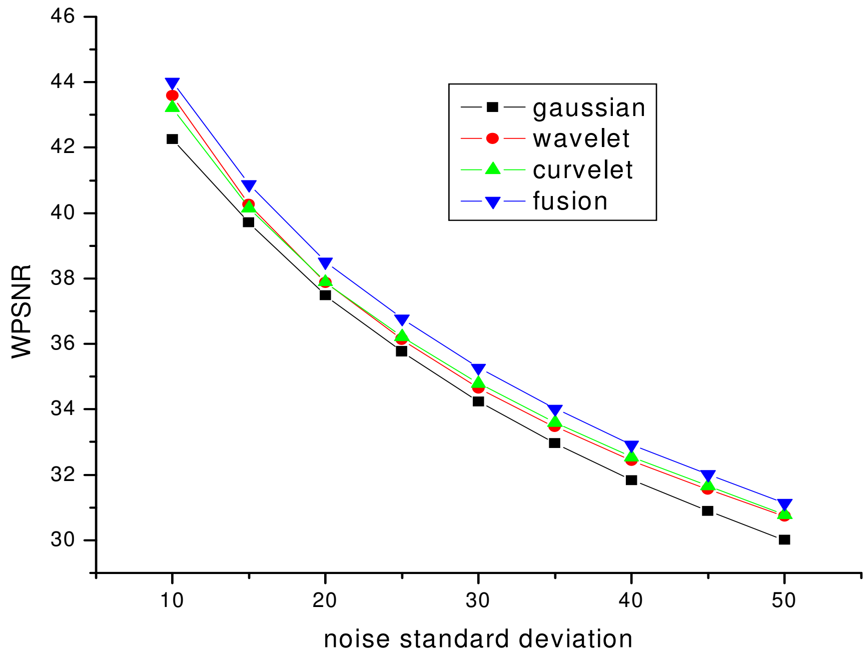

FIGURE 6: WPSNR versus noise standard deviation for four denoising methods on MRI test image

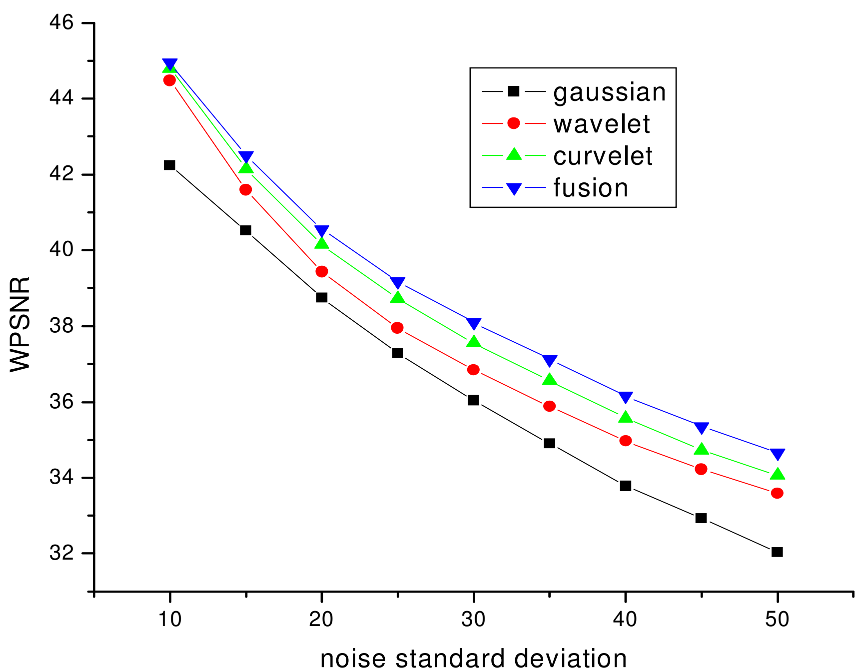

FIGURE 7: WPSNR versus noise standard deviation for four denoising methods on Lena test image

For the four standard images shown below, the comparison of denoising performance in terms of WPSNR is given in the Figure 8

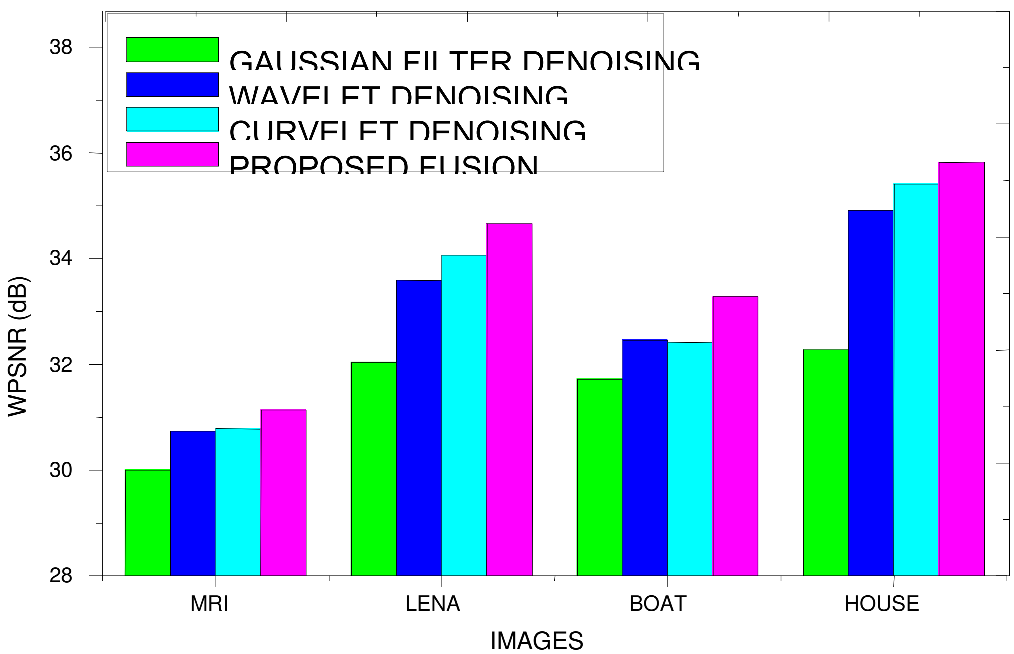

FIGURE 8: Comparison of denoising performance (WPSNR) for four standard images using four denoising methods discussed in this paper.

Though wavelets are well suited to point singularities, they have limitations with orientation selectivity hence do not represent changing geometric features along edges effectively. Curvelet transform exhibits good reconstruction of the edge data by incorporating a directional component to the traditional wavelet transform.

From figure 2,figure 3 and figure 4, we can find out that image (c)is the smoothed version of noisy image after Gaussian filtering which retains most of the noise where as image (d) lost partial edge information after wavelet denoising, the hat's outer edge and ribbon edge and soon become blurred, on the contrary, every edge of image (e) which is denoised by Curvelet transform maintains very well, but appears slight "ringing" phenomenon, appears slight "scratches" phenomenon in the face and hat body and some smooth area. Regardless of losting edge information and "scratches" and "ringing" phenomenon, we do not hope them to appear. Comparatively, image (f) denoised by the fusion of images (c),(d) and (e) we can not only maintain the edge information but also reduce "scratches" and "ringing" phenomenon. On the whole, the fusion method obtained better denoising results than curvelet transform and two-dimensional wavelet transform individually.

4. CONCLUSION

We tested four denoising methods such as Bayes thresholding based wavelet denoising, curvelet transform denoising, Gaussian filtering, and fusion based denoising. Though “scratches” and “ringing” phenomenon are appearing by using traditional Curvelet transform for denoising, we proposed the fusion based method using images after curvelet, wavelet transforms and Gaussian filtering. Our method applies two-dimensional wavelet transform, curvelet transform and Gaussian filtering. After two-dimensional wavelet transform, edge and detail information lost mostly. After curvelet transform, detail information retained better than wavelet transform, meanwhile in denoising process emerged the ringing and radial stripe. After Gaussian filtering image is smoothed to a great extent reducing high frequency noise. So thus with the fusion of three images obtained from the methods discussed we obtained better denoised image by preserving edges and removing Gaussian noise to a great extent and the experimental results prove that the proposed Fusion algorithm is also well suits for medical images as well.

5. REFERENCES

[1].M V S Grace Chang, Bin Yu. “Adaptive wavelet thresholding for image denoising and compression”, *IEEE Transactions on Image Processing*, Vol.9 (9), Sep 2000, pp.1532-1546.

[2]. E.J.Candes, “Ridgelets: Theory and applications, Department of Statistics”, Stanford University, pp.1998, 23-38.

[3].E.J.Candes,” Monoscale Ridgelets for the Representation of Image with Edges”, Department of Statistics, Stanford University, Stanford,CA,1999, pp.1-26.

[4]. J.L. Startck, E.J. Candes, D.L. Donoho, “The curvelet transform for image denoising,” *IEEE Transactions on Image Processing*, Vol.11 (6), 2002, pp.670-684.

[5]. E.J.Candes and D.Donoho, “Curvelet: a surprisingly effective non adaptive representation for object with edges”, Proceeding of Curves and Surfaces IV, France, 1999, pp.105-121.

[6]. David L.Donoho & Mark R.Duncan,”Digital Curvelet Transform: Strategy, Implementation and Experiments”, Department of statistics, Stanford University, Nov 1999, pp.1-20.

[7]. J.Fadili, J.L.Starck, “Curvelets and Ridgelets”, France, Oct 24, 2007, pp.1-30.

[8]. E.Candes, L.Demanet, D.Donoho, L.Ying,”Applied and Computational Mathematics”, Department of Stanford university, Stanford, Mar 2006, pp.1-44.

[9].Anil A.Patil, J.Singhai,” Image Denoising Using Curvelet Transform: an approach for edge preservation”, Journal of scientific and Industrial Research, vol.69, Jan 2010, pp.34-38.

[10].S.G.Mallat,”A theory for Multiresolution signal decomposition: The wavelet representation”, IEEE transactions on Pattern recognition, vol.11, pp. 674-693, 1989.

[11].J.M.Johnstone, D.L.Donoho,”Adapting to smoothness via wavelet shrinkage”, Journal of the Statistical association”, 1995, vol.90, pp.1200-1224.

[12].D.L.Donoho,”Denoising by soft thresholding”, *IEEE transactions on Information theory*, 1995, vol.41, pp.613-627.

[13].D.Donoho and I.Johnstone,"Minimax estimation via wavelet shrinkage", *Annals of statistics*, 1998, vol.26, pp.879-921.

[14].B.Vidakovic,"Statistical modeling by wavelets", John Wiley & Sons, NY, 1999.

[15].I. Daubechies, "Wavelet transforms and orthonormal wavelet bases, different perspectives on wavelets," in *Proceedings of the Symposia in Applied Mathematics*, Vol. 47, pp. 1–33, American Mathematical Society,1993, San Antonio, Tex, USA.

[16].D. L. Donoho, "Ridge functions and orthonormal ridgelets," *Journal of Approximation Theory*, 2001, Vol. 111, no. 2, pp. 143–179.

[17].W. Fourati, F. Kammoun, and M. S. Bouhlel, "Medical image denoising using wavelet thresholding," *Journal of Testing and Evaluation*,2005, Vol. 33, no. 5, pp. 364–369.

[18].M. Do and M. Vetterli, "Image denoising using orthonormal finite ridgelet transform," in *Wavelet Applications in Signal and Image Processing*,2003,vol. 4119 of *Proceedings of SPIE*, pp. 831–842.

[19].L. Demanet, "The curvelet Organization," http://www.curvelet.org/software.html.